ACS OMEGA

Open Access

http://pubs.acs.org/journal/acsodf

Article

Self-Assembly Systems Based on Betaine-Type Hydrophobic Association Polymer Used in Acid Stimulation: Effects of Surfactant and Salt Ion

Yuling Hu, Hongping Quan,* Peng Shen, Xuewen Chen, Yingze Pei, and Zhiyu Huang*

Cite This: *ACS Omega* 2024, 9, 48670−48680

Read Online

ACCESS | Metrics & More | Article Recommendations | Supporting Information

ABSTRACT: Hydrophobic association polymers containing various functional groups have a great deal of application potential as a self-thickening agent in carbonate acidification, while the improvement of their viscosification ability under high temperature conditions remains a significant challenge. A kind of betaine-type hydrophobic association polymer (PASD) intended for use as an acid thickener was synthesized through aqueous solution polymerization with sulfobetaine and a soluble hydrophobic monomer. The structure of PASD was characterized by FT-IR and ^{1}H NMR. It is found that during the acid-rock reaction, the physical cross-linking between PASD and cationic surfactants (STAC) occurs through noncovalent bonding forces such as micellar interaction and electrostatic interaction, forming a self-assembly acid. The optimum conditions for the construction of the self-assembly acid and its viscosification properties, rheological properties, temperature, and salt resistance were evaluated by a six-speed rotating viscometer and a HAAK MARSIII rheometer. The results suggest that the main source of the viscosity rise of the self-assembly acid is the $CaCl_2$ produced during the acid-rock reaction. As the acid-rock reaction progresses, the hydrodynamic radius of the self-assembly acid increases, and tighter aggregation structures form. The viscosity of the self-assembly spent acid still keeps in 140 mPa·s under 140 °C shearing for 1 h at 170 s^{-1}, which indicates that the self-assembly acid has excellent viscosification ability and temperature resistance. Compared to PASD acid, the self-assembly acid can be used at a wider range of temperatures, and its research and development have given rise to novel ideas for the use of HAWPs as an acid thickener.

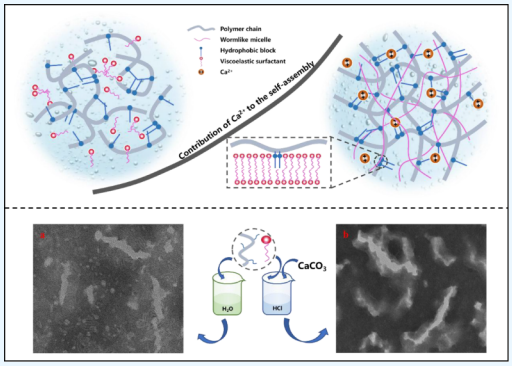

1. INTRODUCTION

With the large-scale development of conventional oil reservoirs, unconventional oil reservoirs have gradually become the focus of petroleum engineers.[1] Among the unconventional oil reservoirs, carbonate reservoirs have huge resource potential, and acidification is an effective measure to increase their production.[2] However, the heterogeneity of carbonate reservoirs causes a large difference in formation permeability,[3] and acid will first enter the high-permeability formation during injection, leaving the low-permeability formation untreated, preventing the acidification operation from producing the best results. As a result, the diversion problem of acid should be considered in the acidification process. Diverting acidification technology can successfully manage this problem by acting as a counterbalance to the flow of acid, allowing formations with varying permeabilities to be acidified equally.

Self-diverting acid composed of acid and chemical admixtures has been extensively investigated in the field of diverting acidification,[4] with viscoelastic surfactant (VES) self-diverting acid being the most commonly used.[5] After Schlumberger introduced a type of quaternary ammonium cationic clean fracturing fluid in 1997, researchers were inspired to create a novel VES acid, which was initially published in the literature in 2001.[6] Numerous studies have up to now examined the gum-breaking, diverting, and viscosification behaviors of various surfactant types in acid.[7−9] The generally recognized mechanism of VES acid is that the changes in concentration of H^+ and Ca^{2+} during the acid-rock reaction can cause the surfactant-formed micelles in the acid solution to transform from globular to wormlike,[10,11] greatly increasing the viscosity of the spent acid, and forcing fresh acid into the formation to flow to the low-permeability formation. Because organic matter, like oil, destroys micelles, VES acid's viscosity naturally decreases after the reaction and backflows easily.[10] However, the viscosity of VES acid can be significantly impacted by a number of additives that are frequently used in acidification operations, such as corrosion inhibitors, iron ion stabilizers, drainage aids, and others.[12,13] Additionally, surfactants are small molecules that must be used in high

Received: August 23, 2024
Revised: October 11, 2024
Accepted: October 24, 2024
Published: November 22, 2024

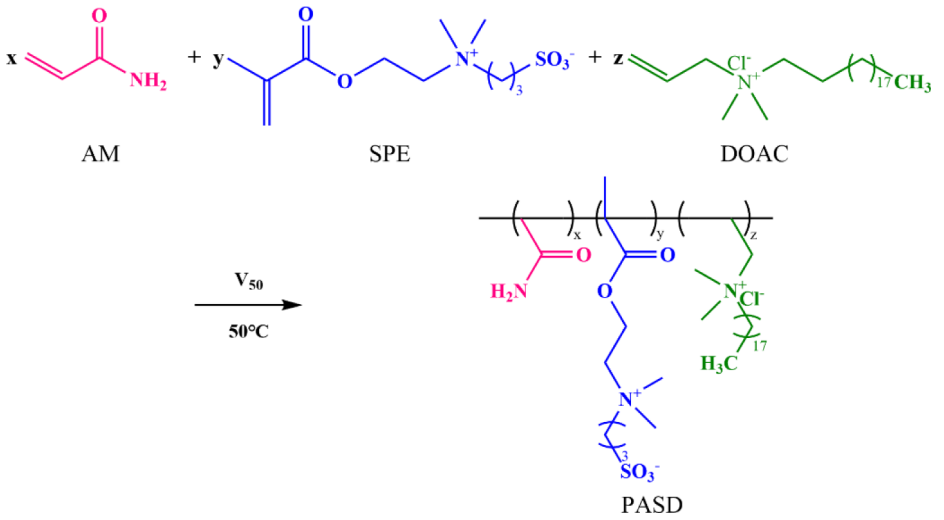

Figure 1. Synthetic route of PASD.

quantities to produce a good performance. In practical applications, it is difficult for VES acid to meet operating requirements at temperatures above 120 °C, and temperature resistance performance needs to be enhanced.

Hydrophobically associating polymers (HAWSPs) have the characteristics of better viscosifying ability, greater viscoelasticity, and greater shearing/temperature/salinity resistance than conventional polymers because of the remarkable hydrophobic interactions and associations between the hydrophobic groups on macromolecular chains. So it is widely used in the field of oil and gas reservoir stimulation.[14−16] Larry Eoff originally proposed the use of hydrophobic association polymers (HAWPs) in the field of diverting acidification in 2004,[17] which can achieve a diverting effect with a tiny amount of HAWPs. Unlike cross-linking polymer self-diverting acid, HAWPs self-diverting acid does not require the addition of cross-linking agents, such as iron salts (Fe^{3+}) or zirconium salts (Zr^{4+}), thereby avoiding the formation damage caused by these agents,[18] which has been widely reported in recent years.[19−21] Nevertheless, there are a few shortcomings with HAWPs acid, including the high viscosity of fresh acid, difficulty pumping into formation, and weak diverting performance at high temperatures.

Surfactants can interact with charge or functional groups carried on HAWPs molecular chains (such as betaine groups and hydrophobic long-chain groups) to produce physical cross-linking structures.[22−25] Based on this concept, aqueous solution polymerization was used to create a betaine-type hydrophobic association polymer (PASD) containing AM, SPE, and DOAC as acid thickeners. The self-assembly behavior of PASD with different types of surfactants was investigated, and the optimal type and amount of surfactant was selected to form self-assembly diverting acid with PASD. The viscosification ability of self-assembly acid is enhanced while maintaining a low viscosity of fresh acid, increasing the temperature adaptation range of PASD. Furthermore, the effect of various salts on the diverting properties of self-assembly acid was investigated, and the thickening mechanism of self-assembly acid was revealed, providing a new concept for the use of HAWPs as an acid thickener.

2. MATERIALS AND METHODS

2.1. Experimental Materials. Acrylamide (AM, ≥98%), 2,2′-azobis (2-methylpropionamidine) dihydrochloride (V50, ≥97%), ethanol (>99.7%), hydrochloric acid (HCl, 36%−38%), stearyl trimethylammonium chloride (STAC, ≥98%), cetyltrimethylammonium chloride (CTAC, ≥99%), dodecyl trimethylammonium chloride (DTAC, ≥99%), sodium dodecyl sulfonate (SDS, ≥98%), sodium hexadecane-1-sulfonate (SHS, ≥98%), calcium carbonate ($CaCO_3$, ≥99%), calcium chloride ($CaCl_2$, ≥97%), magnesium chloride ($MgCl_2$, ≥97%), sodium chloride (NaCl, ≥99.5%), and potassium chloride (KCl, ≥99.5%) were bought from Chengdu Kelong Chemical Factory. *N*, *N*′-dimethyl octadecyl allylammonium chloride (DOAC, ≥70%) was bought from Jiangsu Feixiang Chemical Group. Methyl acrylyl ethyl sulfobetaine (SPE, ≥98%) was purchased from Jiangsu Zhengzhou Alpha Chemical Co., Ltd.

2.2. Synthesis of PASD. Initially, AM (3.9098 g, 0.055 mol), SPE (11.1740 g, 0.040 mol), and DOAC (14.9400 g, 0.040 mol) were dissolved in a 250 mL three-necked flask equipped with a magnetic stirrer. The monomer mass fraction was controlled at 25%,and the pH value of the solution was adjusted to 7−8 with NaOH, then the solution was purged with N_2 for 30 min. Second, after the solution temperature reached 50 °C, initiator V50, whose mass fraction was 0.6% of the total monomer feed, was added, then the polymerization reaction proceeded for 5 h. The PASD was obtained by purification with ethanol and dried at 50 °C under vacuum for 1 day. The synthesis route of PASD is illustrated in Figure 1.

2.3. Reagent Preparation. Diluting concentrated hydrochloric acid (HCl) (36%−38%) to a mass concentration of 20% with pure water, the self-assembly acid system was constructed by adding varying mass ratios of PASD and surfactant to HCl (20%). The $CaCO_3$ required to complete the acid-rock reaction was calculated based on the mass of HCl in the self-assembly acid. $CaCO_3$ was divided into four equal parts and mixed into the self-assembled acid in batches. The reaction was carried out in a water bath at 90 °C until the CO_2 foam completely disappeared after each batch of $CaCO_3$, which means that the $CaCO_3$ reaction was reaction, and then the next batch of $CaCO_3$ was added. Finally, self-assembly

https://doi.org/10.1021/acsomega.4c07784
ACS Omega 2024, 9, 48670−48680

spent acid was obtained. and the acid-rock reaction at different degrees was simulated.

Taking the self-assembly acid containing 200 g of HCl (20%) as an example, the composition changes of the self-assembly acid during the acid-rock reaction are shown in Table 1. It should be noted that the $CaCO_3$ added and CO_2 emitted at each reaction stage are included in the changes in the quality of the solution.

Table 1. Composed of Simulative Self-Assembly Acid During the Acid-Rock Reaction

Mass of HCl (20%)/g	200	–	–	–	–
Dosage of $CaCO_3$/g	0	13.70	27.40	41.10	54.79
Concentration of HCl/wt %	20	14.45	9.29	4.48	~0[a]
Concentration of $CaCl_2$/ wt %	0	7.32	14.13	20.46	26.36

2.4. Characterization and Measurements. *2.4.1. Spectroscopic Characterization.* The structure of PASD was characterized by Fourier transform infrared (FT-IR) and nuclear magnetic resonance (NMR). The FT-IR spectrum was recorded in a KBr pellet with a wavenumber range of 4000−500 cm^{-1} on a WQF-520 Fourier transform infrared spectrophotometer, and the ^1H NMR spectrum in D_2O was performed on Bruker 400 MHz NMR spectrometer, operating at 400 MHz.

2.4.2. Viscosification Law During Acid-Rock Reactions. The viscosity of self-assembly acid under different reaction degrees during the acid-rock reaction was investigated by a six-speed rotational viscometer (ZNN-D6B) at 90 °C and a fixed rotation speed of 100 r·min^{-1}. The sample preparation method is shown in Section 2.3.

2.4.3. Rheology Measurements. Antitemperature performance, steady-state shear, and dynamic oscillation tests were carried out by the rotating rheometer HAAK MARSIII (Thermo Fisher, Germany) to determine the high temperature resistance and rheological performance of the corresponding system. The samples were balanced at room temperature for about 10 min before measurement. The test temperature of steady-state shear and dynamic oscillation was 25 °C, and the test temperature and shear rate of antitemperature performance were 140 °C and 170 s^{-1}, respectively.

2.4.4. Dynamic Light Scattering (DLS). The aggregate sizes of the self-assembly acid at different degrees during the acid-rock reaction were measured by using a laser scatterometer (BI-200SM). Before measurement, the solution was filtered through a 0.45 μm polytetrafluoroethylene filter membrane, and the scattering angle is 90°, the temperature was set at 60 °C. There are two types of samples used for this test: samples containing $CaCl_2$, prepared according to the HCl and $CaCl_2$ composition in Table 1, and samples without $CaCl_2$, prepared according to the HCl composition in Table 1.

2.4.5. Scanning Electron Microscopy (SEM). The apparent morphology of self-assembly acid at different concentrations of Ca^{2+} was observed by Quanta 450 scanning electron microscopy. Moving a drop of sample to the center of the sample table and placing it on the scanning electron microscope workbench after freezing with liquid nitrogen, then the image was recorded when the pressure in the working chamber reached 600−800 Pa. The samples were prepared in pure water and $CaCl_2$ solution.

2.4.6. Transmission Electron Microscopy (TEM). The effect of Ca^{2+} on the aggregation morphology of the system was observed by JEOL JEM 1400 transmission electron microscopy. At a constant temperature of 30 °C and the relative humidity was kept close to saturation, 10 μL of liquid was dropped on a carbon-coated holey film supported by a copper grid, dyed with 1.0 wt % tungsten phosphate, and placed for 1 h. Then the excess solution was removed with filter paper to ensure the evenness of the sample, and the sample was inserted rapidly into liquid ethane (−165 °C) and transferred to liquid nitrogen (−190 °C) for storage. The samples were prepared in pure water and $CaCl_2$ solution.

3. RESULTS AND DISCUSSION

3.1. Characterization of PASD. *3.1.1. FT-IR Spectrum of PASD.* The structure of the obtained copolymer was determined by FT-IR (KBr pellets with optical purity). As shown in Figure 2, the strong absorption peak at 3449 cm^{-1}

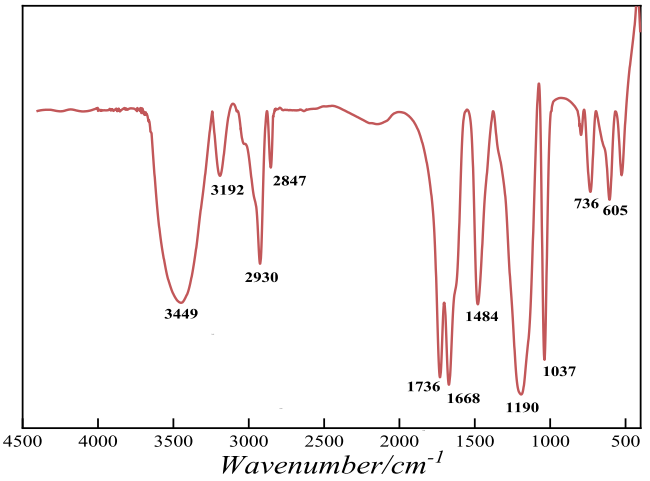

Figure 2. FT-IR spectrum of PASD.

proves the existence of −NH−, the peak at 1668 cm^{-1} is assigned to the stretching vibration of −C═O. The stretching vibration peaks of $-CH_2-$ are observed at 2930 and 2847 cm^{-1}. And the peaks at 1190, 1037, and 736 cm^{-1} are the stretching vibrations from the sulfonic group. The absorption peaks are consistent with those of the functional groups of the target polymer, which indicates that the synthesized product is the expected polymer.

3.1.2. ^1H NMR Spectrum of PASD. To further demonstrate the structure of PASD, the ^1H NMR spectrum of PASD is shown in Figure 3. δ4.70 ppm is the solvent peak (D_2O). The proton signal at 1.76 ppm (1,3,11) belongs to $-CH_2-$ in the main chain of the polymer. The proton signal at 6.19 ppm (2) belongs to $-NH_2$ of AM. The proton signals at 4.55 ppm (5), 3.62 ppm (6), 3.22 ppm (8), 2.53 ppm (9), and 2.28 ppm (10) belong to $-CH_2-$ in different chemical environments of SPE. The proton signals at 1.23 ppm (15) and 0.88 ppm (16) belong to long chain $-(CH_3)_{15}-$ and $-CH_3$, respectively of DOAC. Thus, the ^1H NMR spectrum showed that PASD has been synthesized successfully.

3.2. Effect of Surfactants on the Viscosification Law of PASD Acid During Acid-Rock Reactions. Stearyl trimethylammonium chloride (STAC), cetyltrimethylammonium chloride (CTAC), dodecyl trimethylammonium chloride (DTAC), sodium dodecyl sulfonate (SDS), and sodium

https://doi.org/10.1021/acsomega.4c07784
ACS Omega 2024, 9, 48670−48680

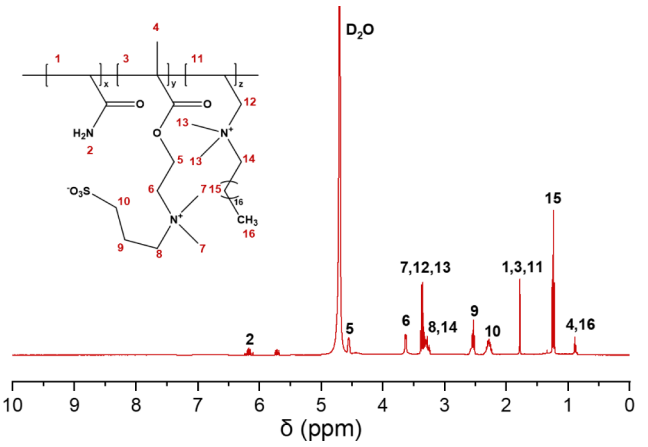

Figure 3. ^{1}H NMR (400 MHz, D_2O) spectra of PASD.

hexadecane-1-sulfonate (SHS) were chosen to form self-assembly systems with PASD acid solution, respectively. The fresh acids were prepared according to method (Section 2.3), and the total mass fraction of PASD and surfactant in the acid solution was 1.2 wt %.

Figures 4 and 5 show the viscosification curves of the PASD acid solution during the acid-rock reaction with varying types and dosages of surfactants. The results indicate that the viscosification ability of the PASD acid solution improves somewhat following the addition of surfactants (regardless of whether they were cationic or anionic), and it peaked at a mass ratio of 1.0:0.2 for PASD to surfactant. When surfactants are added to the PASD acid solutions, surfactant molecules interact with the hydrophobic aggregates of PASD to form mixed micelles,[26,27] and the physical cross-linking network between PASD and micelles will not affect the viscosity of PASD fresh acid, while causing the viscosity of the PASD spent acid to increase significantly. As the surfactant proportion in acid solution increases, the hydrophobe units of PASD gradually distribute into the mixed micelles, and the viscosity of PASD spent acid peaks when the most efficient physical cross-linking network is formed.[28,29] The surfactant proportion increase continues, hydrophobe units are reduced and isolated in different hydrophobic junctions formed by surfactant, which weakens the physical cross-linking network strength between PASD and micelles, and the viscosity of self-assembly spent acid decreases. It is precisely because of the mixed micelles in the self-assembly system that the physical cross-linking network of the spent acid can be affected by water or organic matter in the formation. The viscosity of spent acid will naturally decrease after the acid treatment and backflows easily.

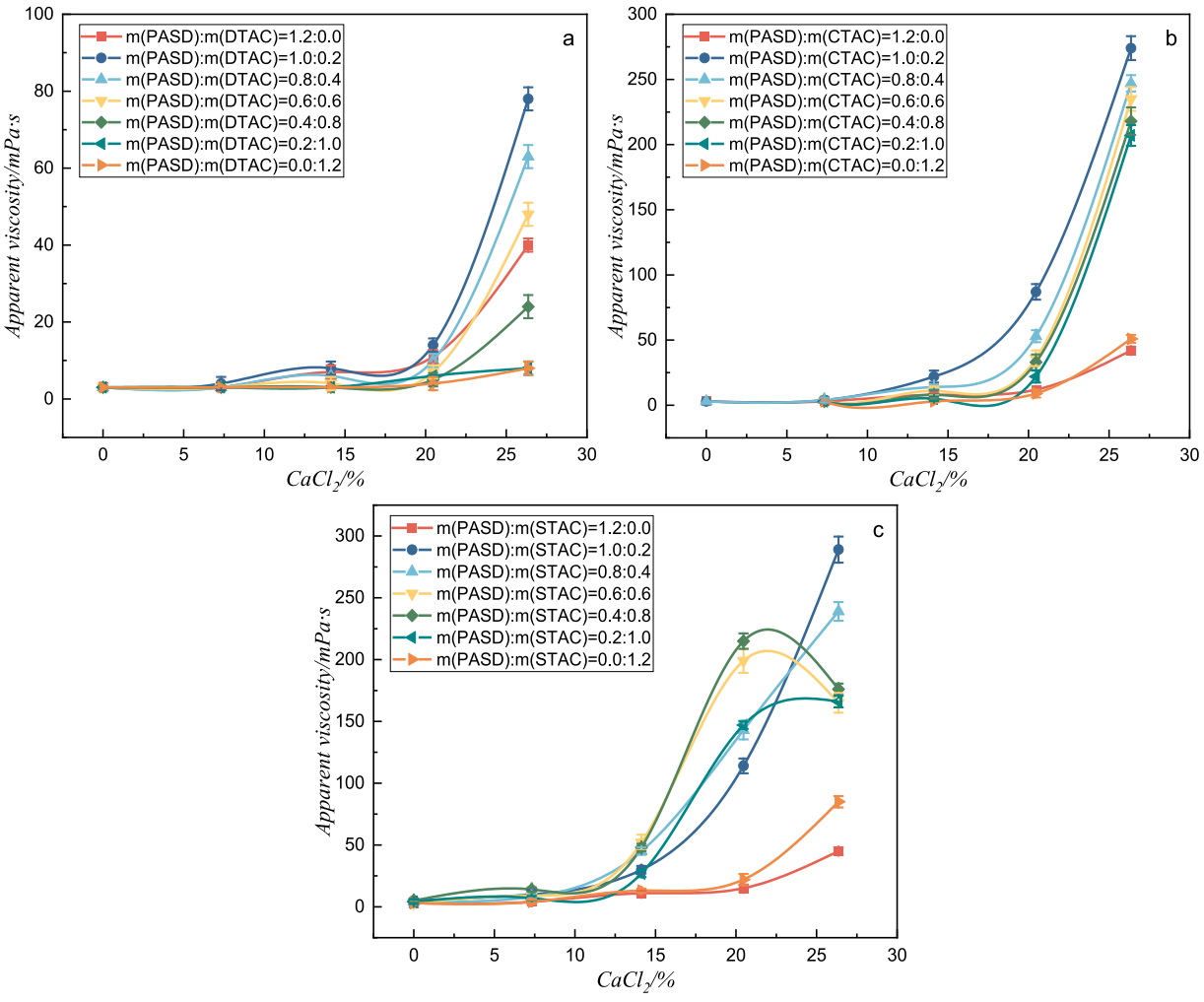

Figure 4. Viscosification law of PASD acid solutions under different kinds and amounts of cationic surfactants (a: DTAC; b: CTAC; c:STAC).

https://doi.org/10.1021/acsomega.4c07784
ACS Omega 2024, 9, 48670−48680

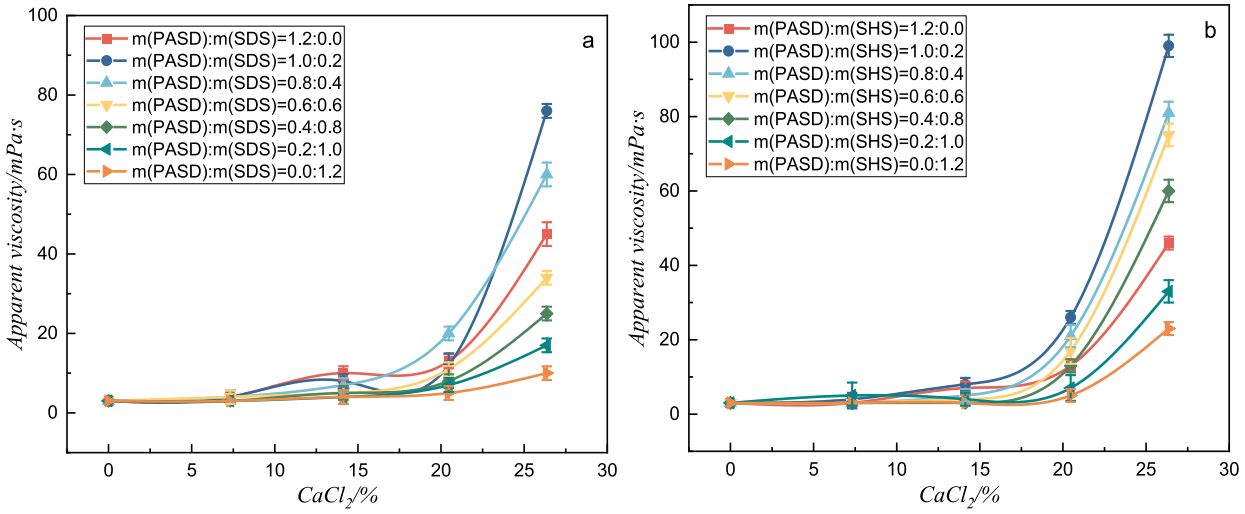

Figure 5. Viscosification law of PASD acid solutions under different kinds and amounts of anionic surfactants (a: SDS; b: SHS).

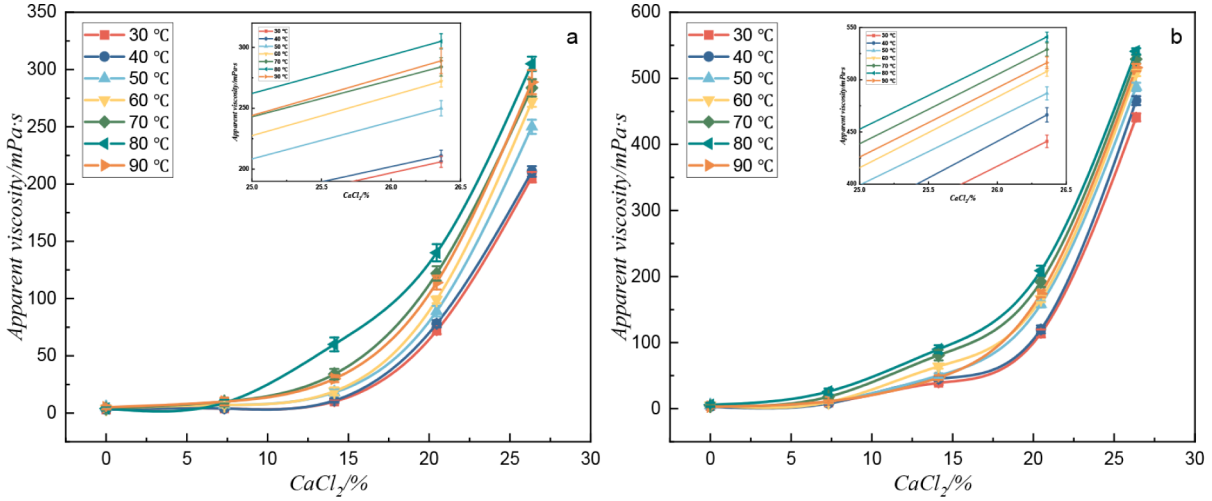

Figure 6. Viscosification ability of self-assembly acid at different temperatures (a: 1.2 wt %; b: 1.5 wt %).

The breaking capability of self-assembly spent acid is shown in Figures S1−S4.

The experimental data in Figure 4 show that the peak viscosity of PASD acid is 42 mPa·s during the acid-rock reaction process, and DTAC, CTAC and STAC increase the peak viscosity of self-assembly acid to 75, 264, and 276 mPa·s, respectively. It means that among the selected surfactants, the longer the surfactant chain length, the better the viscosification ability of PASD acid. Ge et al.[30] studied the effects of betaine surfactants with different chain lengths on the association behavior of associated polymers and reached similar conclusions. The shape of the micelle is determined by the "packing parameter", $V_H/l_c a_0$, so the longer the hydrophobic chain is, the bigger the packing parameter is.[31,32] Surfactant with a bigger packing parameter tends to form worm-like micelles. In the self-assembly system of polymer and surfactant, the more easily the surfactants form worm-like micelles, the more conducive the system to self-assembly into highly viscous fluids. It can be seen from Figures 4b and 5b that the surfactant has the same chain length, cationic surfactants have better viscosification ability than anionic surfactants. CTAC can increase the viscosity to 264 mPa·s, while SHS can increase the viscosity to only 99 mPa·s. The possible reason is the electrostatic effect,[26,33] $-SO_3^-$ in the betaine group of PASD interacted strongly with the cationic surfactant via an electrostatic attraction, which increases the hydrophobicity of PASD.

Besides, Figure 4c shows that the viscosity of PASD spent acid will decrease at the end of the acid-rock reaction when the mass ratio of STAC exceeds 50%. This could be because micellar interaction, rather than hydrophobic association, dominates the viscosity change of self-assembled acid as the mass of STAC increases. While micelles are more prone to inorganic salt destruction, with more $CaCl_2$ produced during the acid-rock reaction, the spatial network structure of self-assembled acids begins to break down and the viscosity of spent acids decreases.

3.3. Temperature Resistance of Self-Assembly Acid.

Previous research revealed that STAC could significantly improve the viscosification ability of PASD acid in the acid-rock reaction process; thus, a self-assembly acid composed of PASD and STAC with a mass ratio of 1.0:0.2 was chosen for the following study. Temperature resistance is an important property of an acidification-working fluid. Figure 6 shows the viscosification ability of self-assembled acid at various temperatures, whereas Figure 7 shows the high-temperature resistance

https://doi.org/10.1021/acsomega.4c07784
ACS Omega 2024, 9, 48670−48680

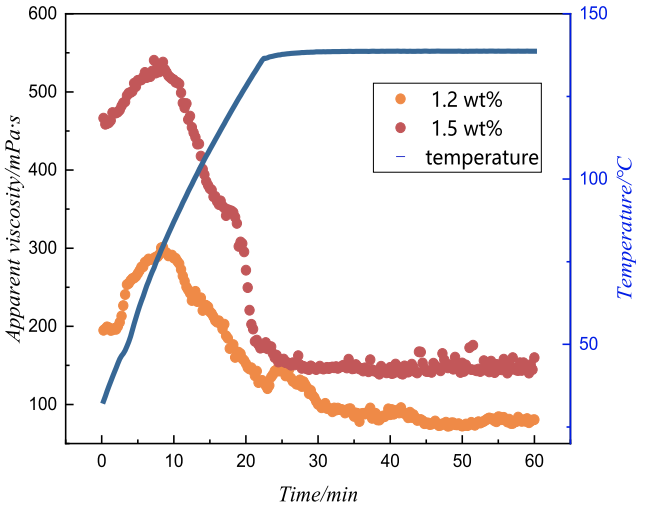

Figure 7. High-temperature rheology of the self-assembly spent acid at 140 °C.

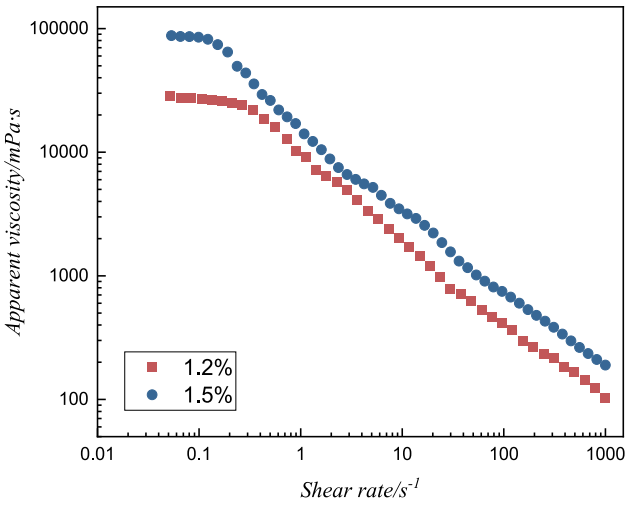

Figure 8. Viscosity curves for self-assembly acids with varying shearing rates.

of self-assembled spent acid. The total mass fractions of PASD and STAC in acid solution were 1.2 and 1.5 wt % (the mass fraction of the self-assembly acid mentioned below is all the sum of PASD and STAC at the mass ratio 1.0:0.2 unless otherwise specified).

As shown in Figure 6, the viscosification ability of self-assembly acid with different dosages exhibits a consistent trend across a range of temperatures; specifically, the viscosification ability becomes better with an increase in temperature (30−80 °C), while decreasing slightly when the temperature exceeds 80 °C. At 30 °C, the peak viscosities of self-assembly spent acid at 1.2 and 1.5 wt % are 206 and 441 mPa·s, respectively. And they increase to 305 mPa·s and 537 mPa·s when the temperature reaches 80 °C. When the temperature rises to 90 °C, the peak viscosities of them still remain at 276 mPa·s and 516 mPa·s. Figure 7 shows the high-temperature rheology of self-assembly spent acid at 140 °C; when the temperature rises from 30 to 90 °C, the viscosity change of self-assembly spent acid is consistent with that shown in Figure 6.

The association between hydrophobic groups is driven by the entropy within a certain temperature range. The interaction between molecular chain segments increases with the increase in temperature,[34−36] which is conducive to the formation of more physical cross-linking points between PASD and STAC, enhanced the degree of entangling between mixed micelles, the spatial network aggregation structure formed by the self-assembly system becomes tighter, and the viscosity of the self-assembly acid increases. However, beyond this temperature, the thermal movement between hydrophobic units and water molecules intensifies with the increase in temperature, weakening the hydrophobic interaction accompanied by shear degradation, which reduces the viscosity of self-assembly acids. After heating for 30 min, the viscosity began to gradually stabilize and finally stay at 80 mPa·s (1.2 wt %) and 140 mPa·s (1.5 wt %), which verified that self-assembly acid has favorable temperature resistance performance.

3.4. Rheological Properties of Self-Assembly Acid.

Steady-state viscosity measurement of self-assembly spent acid with different mass fractions was carried out; viscosity as a function of shear rate for self-assembly spent acid is shown in Figure 8. All solutions are observed to have a narrow Newtonian regime at low shear rates, where the viscosity presents a plateau value and represents a zero-shear viscosity ($\eta 0$). After the Newtonian regime, the viscosity gradually decreases with the increase of shear rate, called shear thinning. Generally, shear thinning is caused by the breakdown of intermolecular forces, including hydrogen bonds, van der Waals forces, and hydrophobic associations. For the self-assembly system formed by PASD and STAC, the hydrophobic chains that bridge the polymer and the mixed micelles are continuously disturbed and rearranged, and the stress experienced by the deformed structure increases with the shear rate.[37,38] After reaching the critical stress, the ends of the bridging chains are pulled out from the entanglement points, the polymer chain and the mixed micelles become entangled at a lower rate than the disentanglement rate, the network structure is destroyed,[23,39−42] and shear thinning behavior is observed.

Figure 9 shows the change curves of the storage modulus (G') and loss modulus (G'') with frequency (Hz) of self-assembly spent acid at different mass fractions. The solutions all show the following pattern: at low frequency, $G'' > G'$, the solution exhibits viscosity behavior, at high frequency, $G' > G''$, the solution exhibits elastic behavior. With the increase of

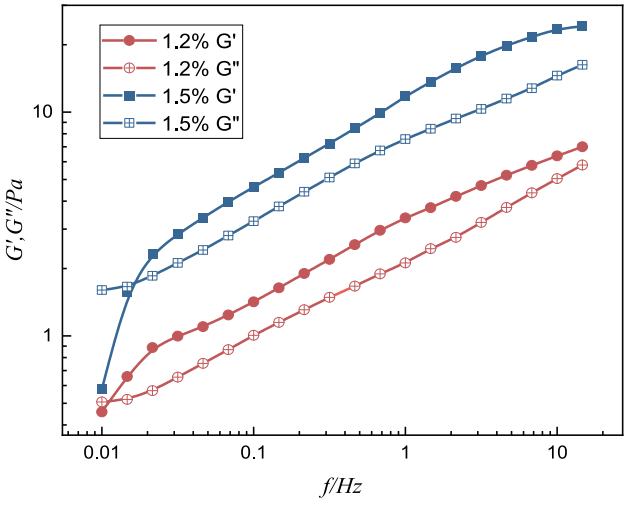

Figure 9. Viscoelasticity measurements for self-assembly acids.

https://doi.org/10.1021/acsomega.4c07784
ACS Omega 2024, 9, 48670−48680

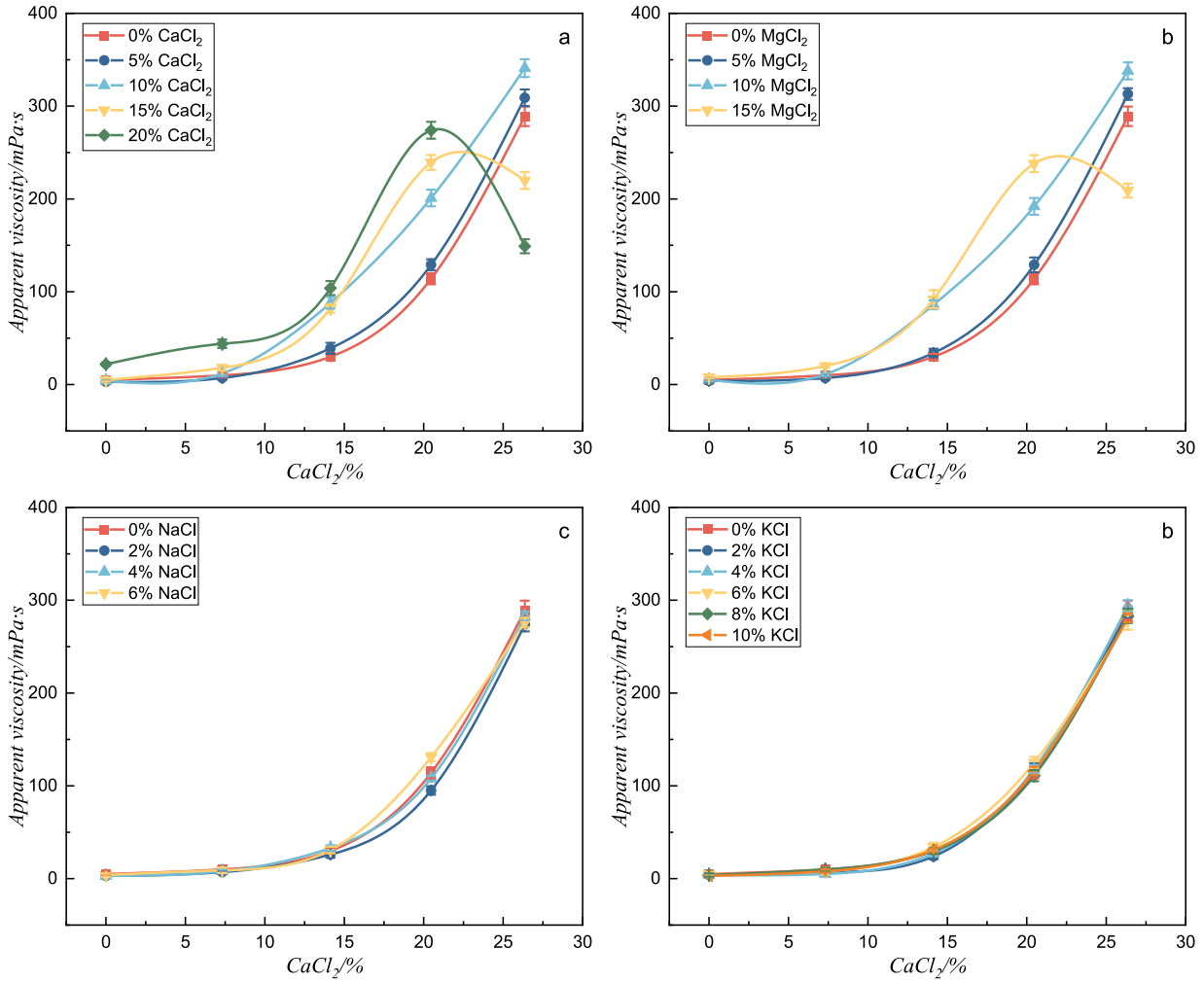

Figure 10. Viscosification ability of 1.2 wt % self-assembly acid at different inorganic salt dosages (a: $CaCl_2$; b: $MgCl_2$; c: NaCl; d: KCl).

frequency (Hz), the storage modulus (G') and loss modulus (G'') of the solutions both increase. The viscoelasticity of PASD/STAC self-assembly system is mainly caused by entanglement between mixed micelles, and the elasticity of the solution is often manifested by the tensile deformation and recovery of molecular chains,[43,44] with the increase of frequency (Hz), the time for molecules in the system to adjust conformational changes to remove stress becomes shorter, and the difficulty of orientation unentanglement for molecular chains becomes more difficult, resulting in the increase of G' and G''.[45]

3.5. Effect of Salt Ion on Self-Assembly Acid. A certain amount of inorganic salt was added to HCl (20%), and then the self-assembled acid was prepared with the salt solution of HCl. The effect of inorganic salt on the viscosification ability of self-assembly acid is shown in Figure 10. The contribution of bivalent salts (Ca^{2+}, Mg^{2+}) to the improvement of the viscosification ability of the self-assembly acid is greater than that of monovalent salts (Na^+, K^+). The addition of salt ions can shield the internal salt bond formed between sulfonic acid groups and quaternary ammonium salt groups in the betaine unit of PASD,[46,47] which makes the molecular conformation of PASD in the acid solution become stretched. The ability to shield the internal salt bond is related to the ionic strength of the salt ion, bivalent salts (Ca^{2+}, Mg^{2+}) have a stronger ability to shield internal salt bonds than monovalent salts (Na^+, K^+).[48] On the other hand, $CaCl_2$ reduces the electrostatic repulsion of the STAC hydrophilic headgroup through Cl^-, decreasing the critical packing parameter and driving STAC to produce wormlike micelles.[48] Besides, the increasing concentration of salt ions continually strengthens the polarity of the solution and promotes the hydrophobic chain of PASD solubilized in the micelle's hydrophobic region, where it forms a mixed micelle network structure with STAC more easily,[49] improving the viscosification ability of self-assembly acid. However, excessive Ca^{2+} and Mg^{2+} will destroy the micellar structure of STAC, which is also the reason why the viscosity of the self-assembly spent acid decreases in the late stage of the acid-rock reaction when the addition of $CaCl_2$ and $MgCl_2$ exceeds 15% (Figure 10a,b).

3.6. Reasonable Mechanism of the Self-Assembly Behavior. Through the experiments in Section 3.5, it is found that bivalent ions can effectively improve the viscosity of the spent acid of the self-assembly system. It can be seen from Table 1 that only H^+ and Ca^{2+} concentration changes in self-assembly acid during the acid-rock reaction. This paper will deeply analyze the main reasons of the viscosity change after the action of carbonate rock and self-assembly acid. In order to analyze the influence law of acid and Ca^{2+} concentration on viscosification ability of self-assembly acid, acid solutions (SAS/HCl) with HCl concentrations of 0%, 4.48%, 9.29%, 14.45%, and 20% were prepared. And the self-assembly acids

https://doi.org/10.1021/acsomega.4c07784
ACS Omega 2024, 9, 48670−48680

($SAS/CaCl_2$) with $CaCl_2$ were prepared by adding $CaCl_2$ corresponding to the HCl concentration in Table 1

The change in apparent viscosity of 1.2 wt % self-assembly acid with different HCl concentrations is presented in Figure 11. It can be seen that the apparent viscosity of SAS/HCl

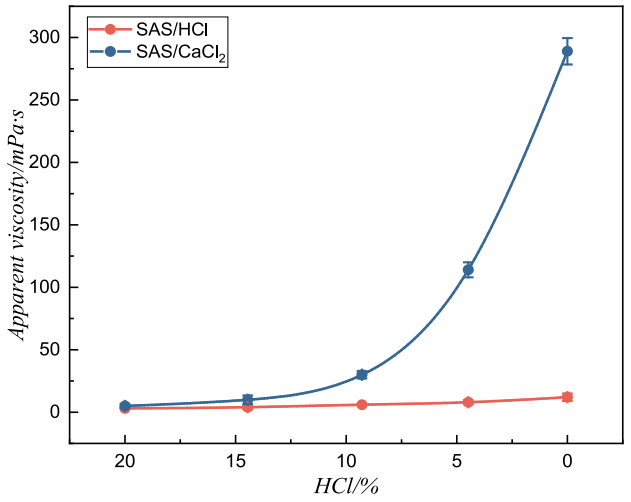

Figure 11. Variation in viscosity of 1.2 wt % self-assembly acid with HCl concentration.

solutions remained relatively unchanged. In contrast, the viscosity of the $SAS/CaCl_2$ solutions increased as the HCl concentration decreased. Combining with the DLS results in Figures 12 and 13, the Rh of self-assembly acid increases with a small growth rate from 70.9 to 236.5 nm as the HCl concentration changes. While in the presence of $CaCl_2$, after the acid-rock reaction, the Rh of the self-assembly acid increased by nearly 60 times (70.9 to 3947.4 nm). It is speculated that high acid concentration increases the charge strength of the headgroup of the surfactant molecule, resulting in the enhancement of intermolecular repulsion force, leading to the increase of the effective area of the headgroup, which is not conducive to the self-assembly of surfactant molecules and polymers. While $CaCl_2$ can enhance the aggregation degree of the mixed micelles, thereby increasing the hydromechanical size of the self-assembly acid,[49−52] Macroscopically, it shows a higher viscosity. These are attributed to the fact that $CaCl_2$ can

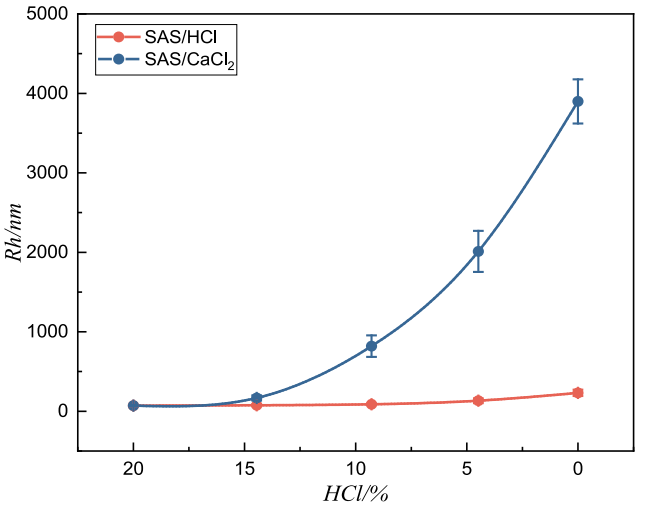

Figure 13. Average Rh of 1.2 wt % self-assembly acid during the acid-rock reaction.

lower the critical packing parameter of STAC, encourage the formation of worm-like micelles,[48] shield the internal salt bond in PASD's molecular structure, and stretch the molecular conformation of PASD.[46,47] It can also increase the polarity of acid solution, make PASD's hydrophobic chains more easily dissolved in STAC micelles, and ultimately enhance the self-assembly ability of the PASD/STAC system.

SEM images provide a more intuitive representation of the phenomenon. In Figure 14a, the self-assembly solution clearly

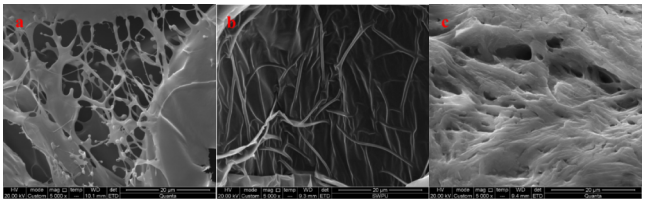

Figure 14. SEM images of 1.2 wt % self-assembly solution (a: 0 wt % $CaCl_2$; b: 14.13 wt % $CaCl_2$; c: 26.26 wt % $CaCl_2$).

displays a linear carbon chain, and a sparse network made up of "thin" side chains is observed. Conversely, Figure 14b shows

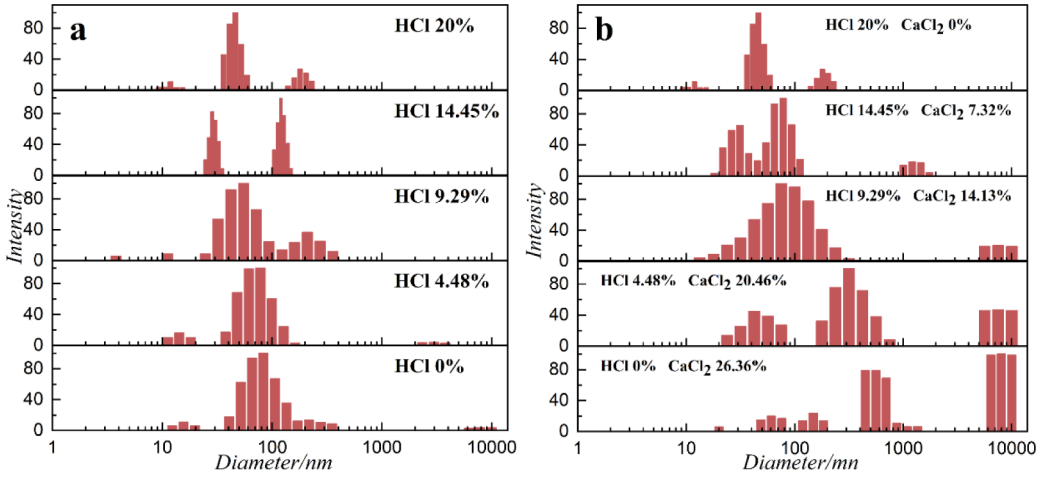

Figure 12. Rh distribution of 1.2 wt % self-assembly acid (a: SAS/HCl; b: $SAS/CaCl_2$).

https://doi.org/10.1021/acsomega.4c07784
ACS Omega 2024, 9, 48670−48680

that the network becomes stronger and denser upon the addition of $CaCl_2$. While the excessive addition of $CaCl_2$ will be adsorbed on the surface of the cross-linking network (Figure 14c), where the network beneath the membrane-like structure is faintly visible.[19]

For further observation of the aggregation form of self-assembly solution at the same $CaCl_2$ concentration in spent acid, the microscopic morphology of a 1.2 wt % self-assembly solution was examined using TEM. As shown in Figure 15, the

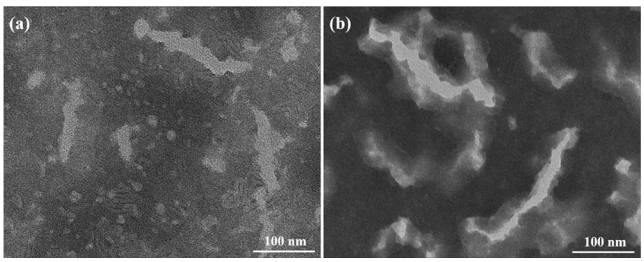

Figure 15. TEM images of 1.2 wt % self-assembly solution (a: 0 wt % $CaCl_2$; b: 26.26 wt % $CaCl_2$).

structure of self-assembly solution aggregates is larger and more complete in the presence of $CaCl_2$, similar to the wormlike micellar aggregation form of surfactant.[53] In the absence of $CaCl_2$, the aggregation structure is more dispersed, like the globular micelle aggregation form of the surfactant. The reasonable mechanism of the self-assembly behavior is shown in Figure 16.

4. CONCLUSIONS

Developed by HMPAM (PASD) and cationic surfactant (STAC), a self-assembly system was obtained by multiple physical cross-linking, including hydrophobic association, electrostatic effect, self-assembly of hydrophobic chains, and worm-like micelles. Compared to the only PASD, the self-assembly system showed unique rheological behaviors and an excellent viscosification ability. With the increase of Ca^{2+} generated during the acid-rock reaction, the self-assembly system formed a denser and stronger mixed micelle network structure in acid, whose hydromechanical radius increased from 70.9 to 3947.4 nm.

The prepared self-assembly spent acid presented the enhanced temperature-resistance ability up to 140 °C; after shearing at 170 s^{-1} for one h, the viscosity of it is maintained at 140 mPa·s. After acid treatment, the physical cross-linked network formed by mixed micelles in self-assembly spent acid will be destroyed by water or organic matter in the formation, the viscosity of the spent acid will naturally decrease and backflow easily. Thus, the self-assembly system can be considered as a novel self-diverting acid that combines the benefits from polymer and surfactant, i.e., better temperature resistance and good fracture cleanup ability, respectively. These unique characteristics confirmed that self-assembly acid has a good application prospect in the field of oil and gas reservoir stimulation.

■ ASSOCIATED CONTENT

Supporting Information

The Supporting Information is available free of charge at https://pubs.acs.org/doi/10.1021/acsomega.4c07784.

Figure S1, viscosity reduction curve of spent acid under the action of H2O; Figure S2, the breaking effect on 1.2 wt% spent acid (left: before breaking; right: after breaking); Figure S3, viscosity reduction curve of spent acid under the action of organic matter; Figure S4, the breaking effect of organic matter on 1.2 wt% spent acid (left: before breaking; right: after breaking) (PDF)

■ AUTHOR INFORMATION

Corresponding Authors

Hongping Quan − *College of Chemistry and Chemical Engineering, Southwest Petroleum University, Chengdu, Sichuan 610500, P. R. China; Oil & Gas Field Applied Chemistry Key Laboratory of Sichuan Province, Chengdu, Sichuan 610500, P. R. China;* orcid.org/0000-0001-5277-7477; Email: quanhp2005@swpu.edu.cn

Zhiyu Huang − *College of Chemistry and Chemical Engineering, Southwest Petroleum University, Chengdu, Sichuan 610500, P. R. China; Oil & Gas Field Applied Chemistry Key Laboratory of Sichuan Province, Chengdu,*

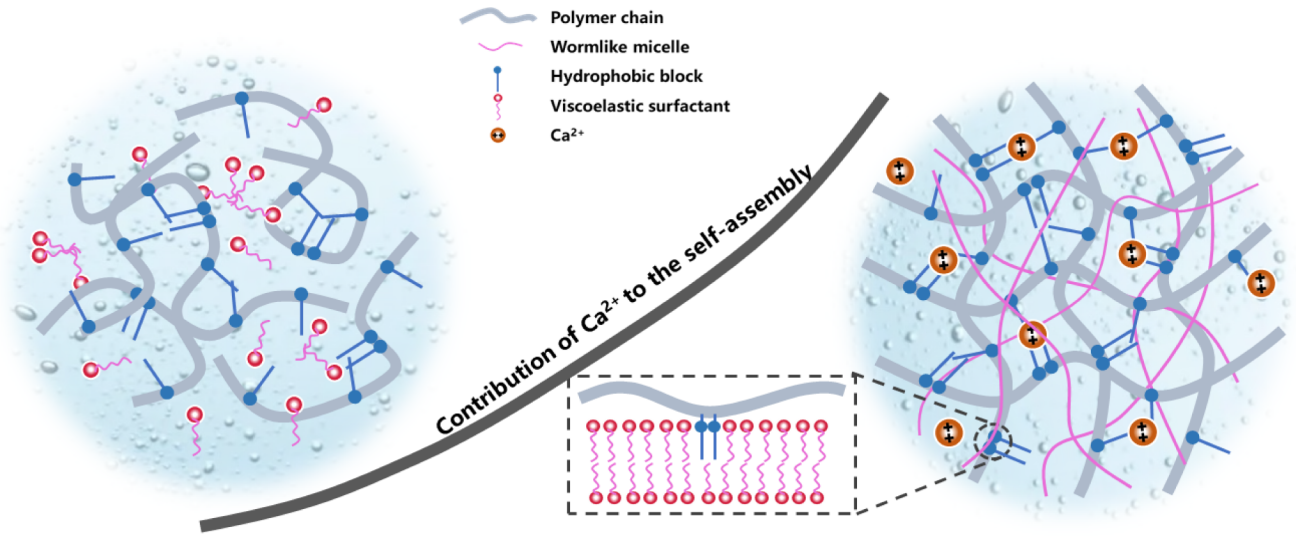

Figure 16. Schematic reasonable mechanism of the self-assembly behavior by the effect of $CaCl_2$.

https://doi.org/10.1021/acsomega.4c07784
ACS Omega 2024, 9, 48670−48680

Sichuan 610500, P. R. China; orcid.org/0000-0002-9115-5571; Email: zyhuang3019@163.com

Authors

Yuling Hu − *College of Chemistry and Chemical Engineering, Southwest Petroleum University, Chengdu, Sichuan 610500, P. R. China; Oil & Gas Field Applied Chemistry Key Laboratory of Sichuan Province, Chengdu, Sichuan 610500, P. R. China*

Peng Shen − *SINOPEC Zhongyuan Petroleum Engineering Design Co., Ltd., Zhengzhou, Henan 450000, P. R. China*

Xuewen Chen − *College of Chemistry and Chemical Engineering, Southwest Petroleum University, Chengdu, Sichuan 610500, P. R. China; Oil & Gas Field Applied Chemistry Key Laboratory of Sichuan Province, Chengdu, Sichuan 610500, P. R. China*

Yingze Pei − *College of Chemistry and Chemical Engineering, Southwest Petroleum University, Chengdu, Sichuan 610500, P. R. China; Oil & Gas Field Applied Chemistry Key Laboratory of Sichuan Province, Chengdu, Sichuan 610500, P. R. China*

Complete contact information is available at: https://pubs.acs.org/10.1021/acsomega.4c07784

Author Contributions

Y.H.: Investigation, conceptualization, methodology, data curation, writing-original draft. H.Q.: Validation, supervision, project administration, funding acquisition. P.S.: Conceptualization, methodology, data curation. X.C.: Investigation, resources. Y.P.: Visualization, formal analysis. Z.H.: Supervision, project administration.

Notes

The authors declare no competing financial interest.

■ ACKNOWLEDGMENTS

This work was supported by the Opening Project of Oil & Gas Field Applied Chemistry Key Laboratory of Sichuan Province (YQKF202001, YQKF201401), Central Guide Local Science and Technology Development Project of Sichuan Province (2023ZYD0031), and Research and Innovation Fund for Graduate Students of Southwest Petroleum University (2022KYCX094).

■ REFERENCES

(1) Malozyomov, B. V.; Martyushev, N. V.; Kukartsev, V. V.; Tynchenko, V. S.; Bukhtoyarov, V. V.; Wu, X.; Tyncheko, Y. A.; Kukartsev, V. A. Overview of Methods for Enhanced Oil Recovery from Conventional and Unconventional Reservoirs. *Energies* **2023**, *16* (13), 4907.

(2) Sarhan, M. A. Editorial: Advanced Techniques and Applications for Characterizing the Hydrocarbon Potential in Carbonate Reservoirs. *Front. Earth Sci.* **2024**, *12*, 1385645.

(3) Martyushev, D. A.; Davoodi, S.; Kadkhodaie, A.; Riazi, M.; Kazemzadeh, Y.; Ma, T. Multiscale and Diverse Spatial Heterogeneity Analysis of Void Structures in Reef Carbonate Reservoirs. *Geoenergy Sci. Eng.* **2024**, *233*, 212569.

(4) Jora, M. Z.; de Souza, R. N.; da Silva Barbosa, M.; Speglich, C.; Sabadini, E. pH-Responsive Wormlike Micelles for Acid Stimulation in Carbonate Reservoirs. *J. Pet. Sci. Eng.* **2022**, *218*, 110975.

(5) Zhao, L.; Chen, X.; Zou, H.; Liu, P.; Liang, C.; Zhang, N.; Li, N.; Luo, Z.; Du, J. A Review of Diverting Agents for Reservoir Stimulation. *J. Pet. Sci. Eng.* **2020**, *187*, 106734.

(6) Chang, F.; Qu, Q.; Frenier, W. A novel self-diverting-acid developed for matrix stimulation of carbonate reservoirs. *SPE International Symposium on Oilfield Chemistry*, Houston, Texas, February 2001; DOI: 10.2118/65033-MS.

(7) Zhang, W.; Mao, J.; Yang, X.; Zhang, H.; Yang, B.; Zhang, Z.; Zhang, Y.; Zhao, J. Development of a Stimuli-Responsive Gemini Zwitterionic Viscoelastic Surfactant for Self-Diverting Acid. *J. Surfactants Deterg.* **2019**, *22* (3), 535−547.

(8) Bulgakova, G. T.; Kharisov, R. Y.; Pestrikov, A. V.; Sharifullin, A. R. Experimental Study of a Viscoelastic Surfactant-Based in Situ Self-Diverting Acid System: Results and Interpretation. *Energy Fuels* **2014**, *28* (3), 1674−1685.

(9) El-Dossoki, F. I.; Abdalla, N. S. Y.; Gomaa, E. A.; Hamza, O. K. An Insight into Thermodynamic and Association Behaviours of Cocamidopropyl Betaine (CAPB) Surfactant in Water and Water−Alcohol Mixed Media. *SN Appl. Sci.* **2020**, *2* (4), 690.

(10) Liu, M.; Zhang, S.; Mou, J.; Zhou, F.; Shi, Y. Diverting Mechanism of Viscoelastic Surfactant-Based Self-Diverting Acid and Its Simulation. *J. Pet. Sci. Eng.* **2013**, *105*, 91−99.

(11) Zhao, Z.; Lue, G. Visco-Elastic Properties of VES Diverting Acid for Carbonate Reservoirs. *Chin. J. Chem. Eng* **2010**, *18* (3), 511−514.

(12) Bybee, K. Interactions of Iron and Viscoelastic Surfactants: A New Formation-Damage Mechanism. *J. Pet. Technol.* **2008**, *60* (6), 72−74.

(13) Vafakish, B. Study of the Rheological Behavior of a Spent Solution of Viscoelastic Surfactant in the Presence of Iron Ions. *Tenside, Surfactants, Deterg.* **2019**, *56* (4), 333−336.

(14) Pal, N.; Vajpayee, M.; Mandal, A. Cationic/Nonionic Mixed Surfactants as Enhanced Oil Recovery Fluids: Influence of Mixed Micellization and Polymer Association on Interfacial, Rheological, and Rock-Wetting Characteristics. *Energy Fuels* **2019**, *33* (7), 6048−6059.

(15) Alves, L.; Lindman, B.; Klotz, B.; Böttcher, A.; Haake, H.-M.; Antunes, F. E. Controlling the Swelling and Rheological Properties of Hydrophobically Modified Polyacrylic Acid Nanoparticles: Role of pH, Anionic Surfactant and Electrolyte. *Colloids Surf., A* **2014**, *459*, 233−239.

(16) Yang, H.; Zhang, H.; Zheng, W.; Zhou, B.; Zhao, H.; Li, X.; Zhang, L.; Zhu, Z.; Kang, W.; Ketova, Y. A.; Galkin, S. V. Effect of Hydrophobic Group Content on the Properties of Betaine-Type Binary Amphiphilic Polymer. *J. Mol. Liq.* **2020**, *311*, 113358.

(17) Eoff, L.; Dalrymple, D.; Reddy, B. R. Development of Associative Polymer Technology for Acid Diversion in Sandstone and Carbonate Lithology. *SPE Prod. Facil.* **2005**, *20* (20), 250−256.

(18) Gomaa, A. M.; Nasr-El-Din, H. A. Effect of Elastic Properties on the Propagation of Gelled and In-Situ Gelled Acids in Carbonate Cores. *J. Pet. Sci. Eng.* **2015**, *127*, 101−108.

(19) Tian, H.; Quan, H.; Huang, Z. Investigation on Rheological Properties and Thickening Mechanism of a Novel Thickener Based on Hydrophobically Associating Water-Soluble Polymer during the Acid Rock Reaction. *J. Pet. Sci. Eng.* **2020**, *188*, 106895.

(20) Quan, H.; Zhen, X.; Wu, Y.; Duan, W. Effect of Non-Crosslinked Polymer (ADDA) on Acid-Rock Reactions: Synthesis and Thickening Laws. *J. Polym. Res.* **2022**, *29* (5), 160.

(21) Tian, H.; Quan, H.; Huang, Z.; Duan, W.; Deng, S. Polymeric and Non-Crosslinked Acid Self-Thickening Agent Based on Hydrophobically Associating Water-Soluble Polymer during the Acid Rock Reaction. *J. Appl. Polym. Sci.* **2019**, *136* (36), 47907.

(22) Tian, H.; Quan, H.; Huang, Z.; Duan, W. Effects of Two Kinds of Viscoelastic Surfactants on Thickening and Rheological Properties of a Self-Thickening Acid. *J. Pet. Sci. Eng.* **2021**, *197*, 107962.

(23) Pu, W.; Du, D.; Liu, R. Preparation and Evaluation of Supramolecular Fracturing Fluid of Hydrophobically Associative Polymer and Viscoelastic Surfactant. *J. Pet. Sci. Eng.* **2018**, *167*, 568−576.

(24) Shakhvorostov, A. V.; Nurakhmetova, Z. A.; Seilkhanov, T. M.; Nuraje, N.; Kudaibergenov, S. E. Self-Assembly of Hydrophobic Polybetaine Based on (Tridecyl)Aminocrotonate and Methacrylic Acid. *Polym. Sci., Ser. C* **2017**, *59* (1), 68−76.

(25) Sun, Q.; Hu, F.-T.; Han, L.; Zhu, X.-Y.; Zhang, F.; Ma, G.-Y.; Zhang, L.; Zhou, Z.-H.; Zhang, L. The Synergistic Effects between

Sulfobetaine and Hydrophobically Modified Polyacrylamide on Properties Related to Enhanced Oil Recovery. *Molecules* **2023**, *28* (4), 1787.
(26) Chen, S.; Han, M.; AlSofi, A. M. Synergistic Effects between Different Types of Surfactants and an Associating Polymer on Surfactant-Polymer Flooding under High-Temperature and High-Salinity Conditions. *Energy Fuels* **2021**, *35* (18), 14484−14498.
(27) Li, G.; Zhou, L.; Wang, C.; Li, E. Study on Self-Assembly Properties of Thermosensitive Fluorinated Hydrophobically Associating Polyacrylamide. *J. Polym. Res.* **2014**, *21* (8), 522.
(28) Das, A.; Chauhan, G.; Verma, A.; Kalita, P.; Ojha, K. Rheological and Breaking Studies of a Novel Single-Phase Surfactant-Polymeric Gel System for Hydraulic Fracturing Application. *J. Pet. Sci. Eng.* **2018**, *167*, 559−567.
(29) Philippova, O. E.; Molchanov, V. S. Enhanced Rheological Properties and Performance of Viscoelastic Surfactant Fluids with Embedded Nanoparticles. *Curr. Opin. Colloid Interface Sci.* **2019**, *43*, 52−62.
(30) Ge, J.-J.; Zhang, T.-C.; Pan, Y.-P.; Zhang, X. The Effect of Betaine Surfactants on the Association Behavior of Associating Polymer. *Pet. Sci.* **2021**, *18* (5), 1441−1449.
(31) Chu, Z.; Dreiss, C. A.; Feng, Y. Smart Wormlike Micelles. *Chem. Soc. Rev.* **2013**, *42* (17), 7174−7203.
(32) Rosen, M. J.; Kunjappu, J. T. *Surfactants and Interfacial Phenomena*, 4th ed.; John Wiley & Sons, Inc, NJ, 2012.
(33) Zhang, X.; Yang, H.; Wang, P.; Zhu, T.; Wang, T.; Chen, C.; Wang, F.; Kang, W. Construction and Thickening Mechanism of Amphiphilic Polymer Supramolecular System Based on Polyacid. *J. Mol. Liq.* **2019**, *286*, 110921.
(34) Li, P.; Wang, L.; Lai, X.; Gao, J.; Dang, Z.; Wang, R.; Mao, F.; Li, Y.; Jia, G. Two-Level Self-Thickening Mechanism of a Novel Acid Thickener with a Hydrophobic-Associated Structure during High-Temperature Acidification Processes. *Polymers* **2024**, *16* (5), 679.
(35) Quan, H.; Hu, Y.; Huang, Z.; Wenmeng, D. Preparation and Property Evaluation of a Hydrophobically Modified Xanthan Gum XG-C16. *J. Dispers. Sci. Technol.* **2019**, *41* (5), 656−666.
(36) Wenfeng, J.; Chenggang, X.; Bao, J.; Junwen, W. A High Temperature Retarded Acid Based on Self-Assembly of Hydrophobically Associating Polymer and Surfactant. *J. Mol. Liq.* **2023**, *370*, 121017.
(37) Rosti, M. E.; Takagi, S. Shear-Thinning and Shear-Thickening Emulsions in Shear Flows. *Phys. Fluids* **2021**, *33* (8), 083319.
(38) Zhang, Y.; Mao, J.; Zhao, J.; Yang, X.; Xu, T.; Lin, C.; Mao, J.; Tan, H.; Zhang, Z.; Yang, B.; Ma, S. Preparation of a Hydrophobic-Associating Polymer with Ultra-High Salt Resistance Using Synergistic Effect. *Polymers* **2019**, *11* (4), 626.
(39) Mahmad Rasid, I.; Ramirez, J.; Olsen, B. D.; Holten-Andersen, N. Understanding the Molecular Origin of Shear Thinning in Associative Polymers through Quantification of Bond Dissociation under Shear. *Phys. Rev. Mater.* **2020**, *4* (5), 055602.
(40) Deblais, A.; Woutersen, S.; Bonn, D. Rheology of Entangled Active Polymer-Like T. *Tubifex Worms. Phys. Rev. Lett.* **2020**, *124* (18), 188002.
(41) Dong, Z.; Li, Y.; Lin, M.; Li, M. Rheological Properties of Polymer Micro-Gel Dispersions. *Pet. Sci.* **2009**, *6* (3), 294−298.
(42) Peng, Y.; Yue, T.; Li, S.; Gao, K.; Wang, Y.; Li, Z.; Ye, X.; Zhang, L.; Liu, J. Rheological and Structural Properties of Associated Polymer Networks Studied via Non-Equilibrium Molecular Dynamics Simulation. *Mol. Syst. Des. Eng.* **2021**, *6* (6), 461−475.
(43) Xie, Y.; Cheng, W.; Yu, H.; Yang, X. Effect of Self-Diverting Acid Viscosity and the Chemical Structure of Coal under Different Acid Environment. *Powder Technol.* **2022**, *398*, 117125.
(44) Ng, W. K.; Tam, K. C.; Jenkins, R. D. Rheological Properties of Methacrylic Acid/Ethyl Acrylate Co-Polymer: Comparison between an Unmodified and Hydrophobically Modified System. *Polymer* **2001**, *42* (1), 249−259.
(45) Zhang, Y.; Mao, J.; Xu, T.; Zhang, Z.; Yang, B.; Mao, J.; Yang, X. Preparation of a Novel Fracturing Fluid with Good Heat and Shear Resistance. *RSC Adv.* **2019**, *9* (3), 1199−1207.
(46) Yang, H.; Zhang, H.; Zheng, W.; Li, X.; Wang, F.; Li, X.; Zhang, D.; Turtabayev, S.; Kang, W. Research on Synthesis and Salt Thickening Behavior of a Binary Copolymer Amphiphilic Polymer. *J. Pet. Sci. Eng.* **2021**, *204*, 108713.
(47) Che, Y.-J.; Tan, Y.; Cao, J.; Xu, G.-Y. Aggregation Behavior of Copolymer Containing Sulfobetaine Structure in Aqueous Solution. *J. Macromol. Sci. Part B* **2010**, *49* (4), 695−710.
(48) Rashidi, M.; Blokhus, A. M.; Skauge, A. Viscosity Study of Salt Tolerant Polymers. *J. Appl. Polym. Sci.* **2010**, *117* (3), 1551−1557.
(49) Xie, Y.; Cheng, W.; Yu, H. Study on Viscosification Law of OAPB Self-Diverting Acid by Acid Concentration and Inorganic Salt in Coal. *Fuel* **2022**, *317*, 123545.
(50) Tian, H.; Shi, Y.; Quan, H.; Huang, Z. Effect of CaCl2 on the Micromorphology of a Self-Thickening Agent (TZXJ) for Acidizing Diversion. *J. Mol. Liq.* **2024**, *398*, 124303.
(51) Klucker, R.; Munch, J. P.; Schosseler, F. Combined Static and Dynamic Light Scattering Study of Associating Random Block Copolymers in Solution. *Macromolecules* **1997**, *30* (13), 3839−3848.
(52) Lu, H.; Liu, Y.; Wang, B.; Zheng, C.; Huang, Z. Self-Assembling Transition Behavior of a Hydrophobic Associative Polymer Based on Counterion and pH Effects. *Colloids Surf., A* **2016**, *490*, 1−8.
(53) Iatridi, Z.; Tsitsilianis, C. pH Responsive Self Assemblies from an A_n-Core-$(B\text{-}b\text{-}C)_n$ Heteroarm Star Block Terpolymer Bearing Oppositely Charged Segments. *Chem. Commun.* **2011**, *47* (19), 5560−5562.

https://doi.org/10.1021/acsomega.4c07784
ACS Omega 2024, 9, 48670−48680